

## Synthesis and Characterization of 2,4-Dichlorophenoxypropanoic Acid (2,4-DP) Herbicide Interleaved into Calcium-Aluminium Layered Double Hydroxide and the Study of Controlled Release Formulation

Farah Liyana Bohari<sup>1</sup>, Nur Aishah Mohd Noor<sup>1</sup>, Sheikh Ahmad Izaddin Sheikh Mohd Ghazali<sup>1\*</sup>, Nur Nadia Dzulkifli<sup>1</sup>, Is Fatimah<sup>2</sup>, and Nurain Adam<sup>3</sup>

<sup>1</sup>Material, Inorganic, and Olochemistry (MaterInoleo) Research Group, School of Chemistry and Environment, Faculty of Applied Sciences, Universiti Teknologi MARA, Cawangan Negeri Sembilan, Kampus Kuala Pilah, 72000, Negeri Sembilan, Malaysia

<sup>2</sup>Department of Chemistry, Faculty of Mathematics and Natural Sciences, Universitas Islam Indonesia, Kampus Terpadu UII, Jl. Kaliurang Km 14, Sleman, Yogyakarta 55584, Indonesia

<sup>3</sup>Kontra Pharma (M) Sdn Bhd (90082-V) Kotra Technology Centre (Block B) 1, 2 & 3, Industrial Estate, 75250, Jl. Ttc 12, Malacca, Malaysia

\* **Corresponding author:**

tel: +60-64832121

email: sheikhahmadizaddin@uitm.edu.my

Received: March 12, 2022

Accepted: June 17, 2022

DOI: 10.22146/ijc.73546

**Abstract:** The commonly used herbicide in agriculture, namely 2,4-dichlorophenoxypropanoic acid (2,4-DP), is an anionic herbicide used to interleave into the interlayer of calcium-aluminum layered double hydroxide (Ca-Al LDH) employing co-precipitation method to form a new nanohybrid labeled as CAL-2,4DP. The LDH compound serves as a host in supporting the herbicide's controlled release formulation. The effective interleave was investigated by employing a powder X-Ray Diffraction (XRD) pattern at 0.025 M nanocomposite, which revealed that the basal spacing has increased from 8.0 Å to 23.8 Å. The ATR-FTIR spectra further supported the interleaving, where the nitrate peak ( $\text{NO}^-$ ) diminished, and the carboxylate ion ( $\text{COO}^-$ ) band appeared at  $1653\text{ cm}^{-1}$ . The percentage loading of CAL-2,4DP was 71.26%, calculated from the carbon content in the sample. The BET analysis shows that CAL-2,4DP was a mesoporous material relying on nitrogen-desorption isotherms. The release of 2,4-DP ions into the aqueous solutions followed the order of  $\text{PO}_4^{3-} > \text{CO}_3^{2-} > \text{Cl}^-$  with a percentage of 83, 65, and 30%, respectively. This work indicates the successful interleaving process of the 2,4-DP anion and the potential of CAL-2,4DP as an eco-friendly agrochemical that can be beneficial for farmers in minimizing herbicide usage to the environment.

**Keywords:** 2,4-dichlorophenoxypropanoic acid (2,4-DP); interleaved; co-precipitation; LDH; nanoparticles; controlled release

### ■ INTRODUCTION

In the case of weed management, farmers are often concerned with the infestation of weeds that grows on a large scale. Weed infestation results in competition between the unwanted plants and the crops for resources such as water, sunlight, nutrients, and space to survive in the agrosystem. This issue needs to be tackled by farmers as their existence can reduce the crop yield, affecting its quality and marketability. As these concerns mount,

farmers have used chemical herbicides directly to eradicate the weeds. Here, they usually assume that the weeds can be easily controlled at a fast rate. Farmers apply herbicide in higher concentration on the crops, which eventually affect the soil and the environment. Some chemical herbicides can evaporate into the air, contaminate the soil, and reach the surface water through running off, which threaten the aquatic organisms [1].

Layered double hydroxide (LDH) denotes the hydrotalcite-like compounds, which comprise brucite ( $\text{Mg}(\text{OH}_2)$ ) like layers mutilated with interlayer anions [2]. The LDH general formula is  $[\text{M}^{2+}_{1-x}\text{M}^{3+}_x(\text{OH}_2)]^{x+}(\text{A}^{n-})_{x/n}\cdot y\text{H}_2\text{O}$ , in which  $\text{M}^{2+}$  and  $\text{M}^{3+}$  denote the divalent and trivalent cations such as calcium ( $\text{Ca}^{2+}$ ) and aluminum ( $\text{Al}^{3+}$ ) accordingly, meanwhile  $\text{A}^{n-}$  is the interlayer anion [3]. The brucite-like sheets are positively charged, in which some part of the divalent cations can be substituted with the trivalent cations [5-8]. The negative charges reside in the hydrated interlayer to compensate for the positively charged sheets and keep the charges balanced while providing its typical stacked layered structures. The sheet's interlayer could be made up of anions and water molecules [5]. Any types of anions such as nitrate ( $\text{NO}_3^-$ ), carbonate ( $\text{CO}_3^{2-}$ ), and chloride ( $\text{Cl}^-$ ) can be interleaved into the interlayer space due to its high anionic exchange capability and variability of chemical composition, giving rise to widespread applications of LDH in drug delivery for pharmaceutical [9-10], polymer composites [8], acting as a host and controlled release formulations in agriculture [5,11-12].

2,4-Dichlorophenoxypropanoic acid (2,4-DP) (Fig. 1) is used as a plant growth regulator commonly utilized to specifically combat broadleaf weeds in crop plantations, for instance, wheat, rice, and domestic usage [11]. However, 2,4-DP anion (Fig. 2) is highly polar and has high water solubility. Thus, the active substances can be easily released to the surface water and bioaccumulate in the water [5,13-14]. Therefore, due to the unique properties of LDH acting as a host, 2,4-DP herbicide can be interleaved into the LDH interlayer matrix. The interleaving process between the 2,4-DP herbicide and LDH host can reduce the concentration of the released agrochemicals and minimize the environmental impacts by producing the new environmentally friendly herbicide. The intercalation was synthesized using the co-

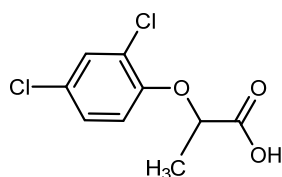


Fig 1. Molecular structure of 2,4-DP

precipitation method because of its simplicity and high yield. The interaction of the 2,4-DP anion and its LDH host was analyzed using the FTIR, XRD, CHNS, and BET techniques, while the controlled release of the active substances was measured using the UV-Vis instrument.

## ■ EXPERIMENTAL SECTION

### Materials

The reagents used in the calcium-aluminum LDH (Ca-Al LDH) interleaving and synthesis procedure were utilized without additional purification. These reagents included calcium nitrate tetrahydrate, ( $\text{Ca}(\text{NO}_3)_2 \cdot 6\text{H}_2\text{O}$ , 99%, R&M Chemicals), Aluminum nitrate nonahydrate, ( $\text{Al}(\text{NO}_3)_3 \cdot 9\text{H}_2\text{O}$ , 98.5%, R&M Chemicals), sodium hydroxide (NaOH, 99%, Merck), 2,4-dichlorophenoxypropanoic acid (2,4-DP) ( $\text{C}_9\text{H}_8\text{Cl}_2\text{O}_3$ , 98.5%, Sigma-Aldrich), and absolute ethanol ( $\text{C}_2\text{H}_5\text{OH}$ , 99.7%, HmbG Chemicals).

### Instrumentation

X-ray powder diffraction (XRD) patterns were recorded at the  $5-90^\circ$  range utilizing a Bruker D8 Advance XRD diffractometer, operating under Cu K $\alpha$  radiation at 40 mA and 40 kV ( $\lambda = 1.54059 \text{ \AA}$ ) with a scanning step of  $0.01^\circ$ . The Fourier transformed infrared (FTIR) spectra were gained on a Perkin Elmer Spectrum 100 utilizing attenuated total reflectance (ATR) mode in the  $4000-650 \text{ cm}^{-1}$  range. The elemental analysis was conducted utilizing a CHNS analyzer, model CHNS-932. The pore size and surface area distribution of the Brunauer-Emmett-Teller (BET) analysis were assessed by employing nitrogen adsorption-desorption of the nanocomposites on a Micromeritics surface area and pore analyzer (ASAP 2000). The controlled release of the 2,4-DP herbicide from the Ca-Al LDH host was assessed utilizing a 0.3 mg sample into a 3.5 mL 0.01 M of various salt solutions of NaCl,  $\text{Na}_2\text{CO}_3$ , and  $\text{Na}_3\text{PO}_4$  [13]. By

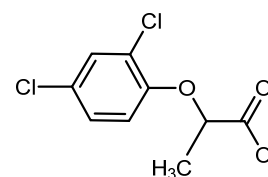


Fig 2. Molecular structure of the 2,4-DP anion

employing a Perkin Elmer UV-Vis Spectrophotometer Lambda 35, the anions produced in the aqueous solutions were monitored for 20 h at a predetermined time.

## Procedure

### Synthesis of calcium-aluminium layered double hydroxide host (Ca-Al LDH)

For the precursors, approximately 0.033 M  $\text{Al}(\text{NO}_3)_3 \cdot 9\text{H}_2\text{O}$  as well as 0.10 M  $\text{Ca}(\text{NO}_3)_2 \cdot 6\text{H}_2\text{O}$  were mixed together into 250 mL of DI water. Following from there, to avoid carbon dioxide ( $\text{CO}_2$ ) contamination, the mixture pH was accustomed to 11 by adding 2 M NaOH followed by vigorous stirring under a nitrogen atmosphere. After that, the mixture went through the aging process for 18 h at 70 °C in an oil bath shaker. Precipitate could be seen in the mixture after 18 h, which was then centrifuged for 25 min at 300 rpm. After centrifugation, the precipitate was removed and washed multiple times with DI water before being dried in an oven at 80 °C for 72 h. Finally, for further usage and characterization, the material was crushed into a fine powder.

### Synthesis of Ca-Al-2,4DP-LDH nanocomposite (CAL-2,4DP)

The intercalation of the 2,4-DP herbicide into the interlayer LDH was done using the co-precipitation method. The same precursors were used according to the synthesis of Ca-Al LDH, followed by adding different concentrations of 125 mL 2,4-DP herbicide in the range of 0.025–0.10 M into the conical flask filled with metal cations mixtures. Then, the solution was stirred under the nitrogen gas purge at a constant pH of 11 using NaOH solution until a white precipitate was formed. The solution was aged, followed by the centrifugation of the precipitate, and dried at 80 °C for 72 h before sample characterization.

## RESULTS AND DISCUSSION

### PXRD Analysis and Spatial Orientation of 2,4-DP

Fig. 3 portrays the PXRD patterns of both the Ca-Al LDH host and its nanocomposite, CAL-2,4DP, at various concentrations in the range of 0.025–0.1 M. The pattern of Ca-Al LDH showed high crystallinity and harmonious peaks, which is consistent with the typical LDH host [7-9, 15]. It also has a well-defined peak at 10.34° corresponding

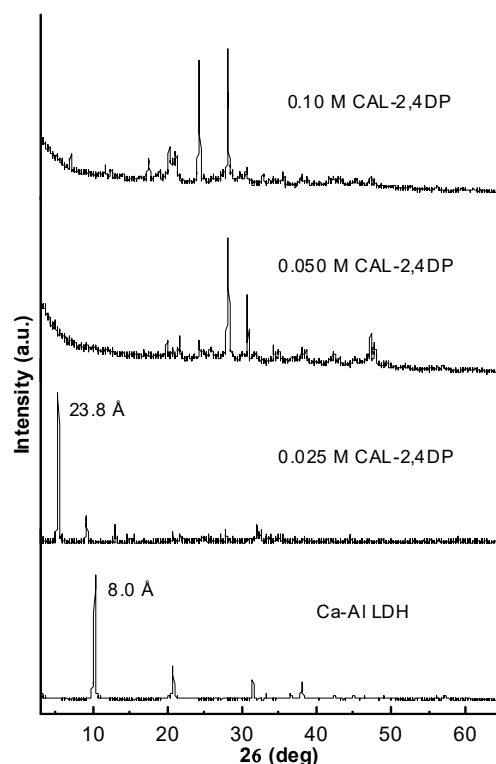
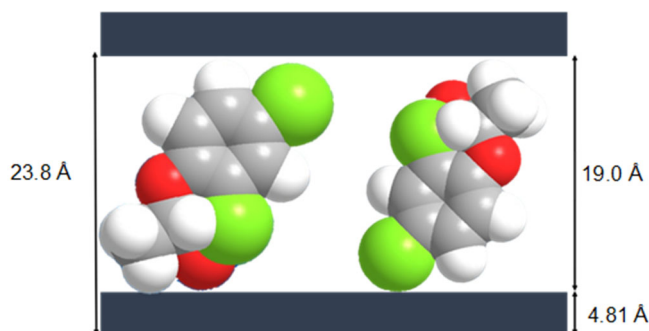


Fig 3. PXRD patterns of Ca-Al LDH and three different concentrations of CAL-2,4DP

to the basal spacing of 8.0 Å, measured utilizing Bragg's law formula. Moreover, as portrayed on 0.025 M CAL-2,4-DP, the diffraction peak of the synthesized nanohybrid can be seen shifting to the lower angle at 3.71°. The basal spacing has expanded from 8.0 to 23.8 Å, indicating that the 2,4-DP anion interleaved into the interlamellar of the LDH host. Here, the difference in the basal spacing is pronounced compared to the LDH host due to the anion size of 2,4-DP, which is larger than the nitrate ions, and the spatial orientation between the interlayers [15]. As discussed, this peak signifies the interleaving of 2,4-DP into the LDH host. However, the PXRD patterns of 0.05 M and 0.1 M CAL-2,4DP showed that the interleaving process did not complete between the guest and the host anions. The presence of carbonate and calcite can be observed near 25° and 29° due to the carbonate contamination [16]. Overall, it could be inferred that the interleaving process occurred at a lower concentration of CAL-2,4DP.

Fig. 4 shows the proposed spatial orientation of 2,4-DP within the Ca-Al LDH using ChemOffice software.



**Fig 4.** Proposed spatial orientation of 2,4-DP in the interlayer of LDH

Based on the basal spacing of CAL-2,4DP, 23.8 Å, the interlayer gallery height for the accommodation of 2,4-DP can be calculated. Taking into account that the thickness of the Ca-Al LDH layer is 4.81 Å [17] implies that the expected gallery height that the 2,4-DP anions can accommodate was 19 Å. Therefore, it can be suggested that the 2,4-DP anions were oriented in bilayer arrangement within the interlayer.

### FTIR Analysis

Fig. 5 shows the FTIR-ATR spectra of the Ca-Al LDH host and its guest. Because of the O-H stretching and bending vibration of the hydroxyl groups in the interlayer water molecules, bands exist at 3460  $\text{cm}^{-1}$  and 1631  $\text{cm}^{-1}$  at Ca-Al LDH [18]. Note that a sharp band at 1325  $\text{cm}^{-1}$  associates with the nitrate stretching vibration. Besides that, a peak of 1443  $\text{cm}^{-1}$  refers to the carbonate stretching in the interlayer region that might be due to the  $\text{CO}_2$  contamination from the air during the preparation [5]. For the FTIR spectra of pure 2,4-DP, the peak at 2912  $\text{cm}^{-1}$  is associated with the stretching vibration of the O-H groups from COOH.

On the other hand, the sharp peak at 1732  $\text{cm}^{-1}$  resembles the carbonyl group (C=O) functional group. Following here, another distinct peak can be seen at 1489  $\text{cm}^{-1}$ , indicating the C=C vibrations of the aromatic ring [19]. Finally, the C-Cl vibration at the aromatic ring can be observed at 817  $\text{cm}^{-1}$ .

The 2,4-DP herbicide was interleaved into the LDH interlayer area according to the FTIR spectra of 0.025 M CAL-2,4DP. The O-H stretching caused by the adsorbed interlayer water molecules produces a broad absorption

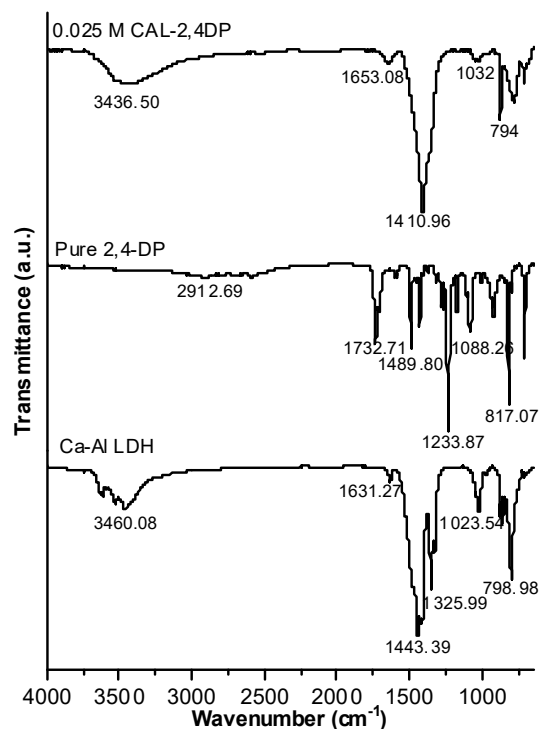


**Fig 5.** FTIR spectra of Ca-Al LDH and its nanocomposite

band at 3436  $\text{cm}^{-1}$ . Moreover, the O-H bending of the COOH is shown by the emergence of a prominent absorption band at 1410  $\text{cm}^{-1}$ , while the carbonyl group may be observed at 1653  $\text{cm}^{-1}$ . Moreover, the interleaved process can be confirmed by vanishing the nitrate peak around 1325  $\text{cm}^{-1}$ , signifying that 2,4-DP anion has already exchanged with the nitrate ions that initially occupied the interlayer host. On the other hand, a peak of 794  $\text{cm}^{-1}$  attributes to the C-Cl attached to the aromatic ring. Thus, based on the spectra for CAL-2,4DP, the nanocomposite resembles the absorption bands in both LDH and 2,4-DP. The FTIR spectrum of CAL-2,4DP suggests that 2,4-DP anion can be interleaved successfully in the interlayer lamellae at a lower concentration.

### Elemental Analysis

Table 1 indicates the elemental analysis of the Ca-Al LDH host and CAL-2,4DP nanocomposite obtained from the CHNS analysis. The result shows that Ca-Al LDH comprises 3.05% nitrogen. The nitrogen content aligns with the occurrence of a sharp band at 1325  $\text{cm}^{-1}$  in the FTIR spectra of Ca-Al LDH (Fig. 5), representing

**Table 1.** Basal spacing and chemical composition of Ca-Al LDH host and its intercalated compound, CAL-2,4DP (0.025 M)

Sample	d (Å)	% C (%w/w)	% H (%w/w)	% N (%w/w)	% loading
Ca-Al LDH	8.0	0.16	2.51	3.05	-
CAL-2,4DP	23.80	25.58	3.74	0.23	71.26

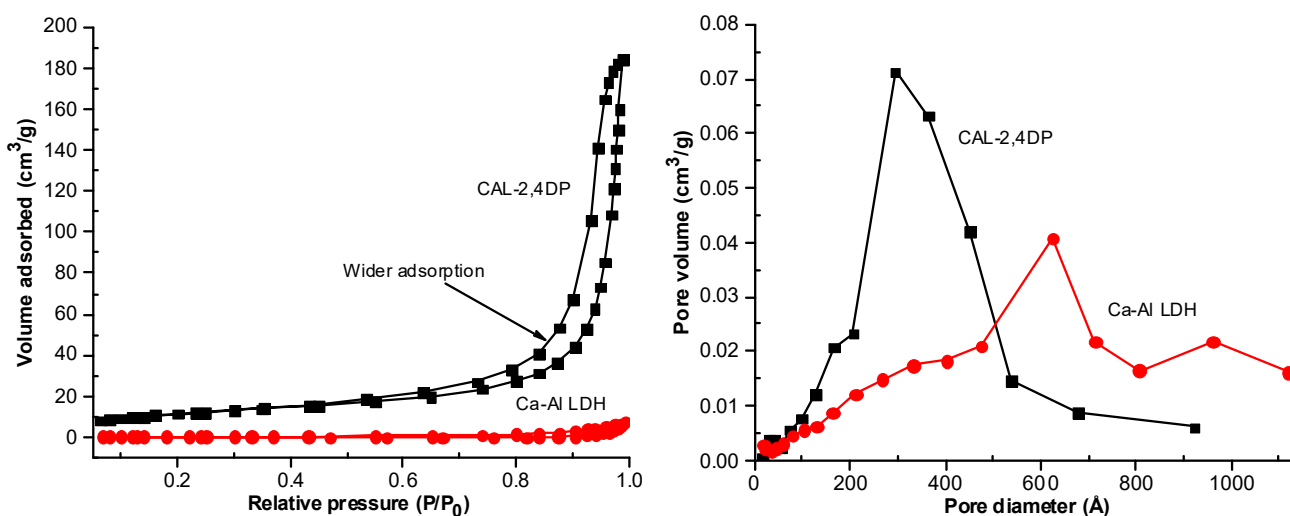
the nitrate group. The percentage content of C and H in the CAL-2,4DP nanocomposite increased due to the presence of a 2,4-DP anion that interleaved into the interlayer. The nitrogen content in the nanocomposite also decreases to 0.23% after the interleaving process. The percentage loading of 2,4-DP intercalated into the Ca-Al LDH interlayer is estimated to be 71.26% based on the carbon content of about 25.58 % in the CAL-2,4DP.

### Surface Properties

The nitrogen adsorption-desorption isotherms and pore size distribution for Ca-Al LDH, along with its intercalated compound, 0.025 M CAL-2,4-DP, are all portrayed in Fig. 6. Depending on the IUPAC (International Union of Pure and Applied Chemistry) categorization, the isotherms resemble Type IV sorption, indicating mesopore-type material with an H3 hysteresis loop [7]. The hysteresis loop for the CAL-2,4DP observed has a broader adsorption branch than the Ca-Al LDH due to the interleaving process of the 2,4-DP anion replacing the nitrate ion. As a result, the adsorbate uptake for CAL-2,4DP increases slowly at a relative pressure of 0.0–0.5,

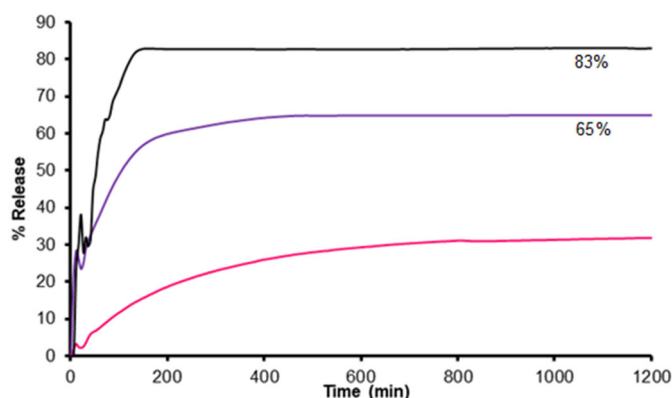
followed by rigorous adsorption at a relative pressure of above 0.7, with maximum uptake at  $184 \text{ cm}^3 \text{ g}^{-1}$ . Nonetheless, Ca-Al LDH portrays a similar pattern of delayed adsorbate uptake at a relative pressure of 0.0–0.8, reaching an optimum uptake at  $9 \text{ cm}^3 \text{ g}^{-1}$ . For the BJH desorption pore size distribution, the interleaved compound of CAL-2,4DP shows higher pore size distribution at about 200–450 Å with a pore volume of  $0.07 \text{ cm}^3 \text{ g}^{-1}$ . Here, the Ca-Al LDH portrays minimal pore volume at  $0.04 \text{ cm}^3 \text{ g}^{-1}$  under 620 Å. Furthermore, the difference in pore structure and distribution for both host-guest relies on the formation of interstitial pores between the size of the particles and crystallite during the interleaving process [20].

Table 2 encapsulates the porosity and surface area of Ca-Al LDH and CAL-2,4DP employing the Brunauer, Emmett, and Teller (BET) and the Barrett, Joyner, and Halenda (BJH) methods. Here, the BET surface area increased from  $17.93 \text{ m}^2 \text{ g}^{-1}$  for Ca-Al LDH to  $21.35 \text{ m}^2 \text{ g}^{-1}$  for CAL-2,4DP. The increase in surface area for CAL-2,4DP indicates that the interleaving process has taken place and agrees with the expansion of basal spacing in

**Fig 6.** Adsorption-desorption isotherm and pore size distribution of Ca-Al LDH and CAL-2,4DP

**Table 2.** Surface properties of Ca-Al LDH and CAL-2,4DP (0.025 M)

Sample	Surface area ( $\text{m}^2 \text{g}^{-1}$ )	BJH desorption pore volume ( $\text{cm}^3 \text{g}^{-1}$ )	BET average pore diameter ( $\text{\AA}$ )	BJH average pore diameter ( $\text{\AA}$ )
Ca-Al LDH	17.93	180.36	94.34	156.71
CAL-2,4DP	21.35	178.59	111.14	126.90

**Fig 7.** Release profiles of 2,4-DP anion from CAL-2,4DP into 0.01 M of various aqueous solutions

in Fig. 3. In addition, the inclusion of larger 2,4-DP anions generates more pores in the crystallites, increasing the surface area for the intercalated compound [21].

### Controlled Release Studies

The release profiles of the accumulated 0.025 M CAL-2,4DP from the Ca-Al LDH interlayer into various aqueous solutions were investigated in Fig. 7. The salt solutions were observed according to their ion charges of phosphate ( $\text{PO}_4^{3-}$ ), carbonate ( $\text{CO}_3^{2-}$ ), and chloride ( $\text{Cl}^-$ ). In the first 15 min, the release patterns of the 2,4-DP anion were rapid, followed by a much slower release upon reaching its equilibrium condition around 200 min. Here, the accumulated 2,4-DP ions depend on the availability of anion in the aqueous solutions following the order of  $\text{PO}_4^{3-} > \text{CO}_3^{2-} > \text{Cl}^-$  with percentages of 83, 65, and 30%, respectively. Phosphate ions with the highest percentage confirm that a higher density charge affects a higher amount of  $\text{PO}_4^{3-}$  anion to be exchanged with 2,4-DP anion [18]. Therefore,  $\text{PO}_4^{3-}$  anions are interleaved into the Ca-Al LDH interlayer during the controlled release process, which simultaneously releases the 2,4-DP ions out from the interlayer into the aqueous solution.

### CONCLUSION

In this study, a new nanohybrid LDH was successfully synthesized through the interleaving process of 2,4-DP herbicide into Ca-Al LDH interlayer via the co-precipitation method. The resulting synthesized nanohybrid, CAL-2,4DP, confirmed its interleaving process through several characterization techniques such as PXRD, FTIR, and elemental analysis. The PXRD analysis portrays the basal spacing expansion from 8.0  $\text{\AA}$  to 23.8  $\text{\AA}$ , implying that the 2,4-DP anion interleaved into the interlayer and replaced the nitrate ions. The synthesized nanohybrid of CAL-2,4DP is proven to be mesoporous material with type IV sorption according to the BET analysis. Moreover, the release of 2,4-DP anion from the Ca-Al LDH host is dependent on the available ions in the aqueous solution in the order of  $\text{PO}_4^{3-} > \text{CO}_3^{2-} > \text{Cl}^-$ . Therefore, this research proposes the Ca-Al LDH possibility as a host carrier for herbicide-controlled release mechanism to decrease the agrochemicals usage in agriculture.

### AUTHOR CONTRIBUTIONS

Farah Liyana Bohari and Nur Aishah Mohd Noor experimented, Nur Nadia Dzulkifli analyzed the data, and Nurain Adam conducted the calculations. Is Fatimah and Sheikh Ahmad Izaddin Sheikh Mohd Ghazali wrote and revised the manuscript. All authors agreed to the final version of this manuscript.

### REFERENCES

- [1] Aktar, W., Sengupta, D., and Chowdhury, A., 2009, Impact of pesticides use in agriculture: Their benefits and hazards, *Interdiscip. Toxicol.*, 2 (1), 1–12.
- [2] Wijitwongwan, R., Intasa-ard, S., and Ogawa, M., 2019, Preparation of layered double hydroxides toward precisely designed hierarchical organization,

- ChemEngineering*, 3 (3), 68.
- [3] Shahabuddin, S., Sarih, N.M., Afzal Kamboh, M., Rashidi Nodeh, H., and Mohamad, S., 2016, Synthesis of polyaniline-coated graphene oxide@SrTiO<sub>3</sub> nanocube nanocomposites for enhanced removal of carcinogenic dyes from aqueous solution, *Polymers*, 8 (9), 305.
- [4] Gonzalez Rodriguez, P., de Ruyter, M., Wijnands, T., and ten Elshof, J.E., 2017, Porous layered double hydroxides synthesized using oxygen generated by decomposition of hydrogen peroxide, *Sci. Rep.*, 7 (1), 481.
- [5] Kim, G., and Park, S., 2021, Chloride removal of calcium aluminate-layered double hydroxide phases: A review, *Int. J. Environ. Res. Public Health*, 18 (6), 2797.
- [6] Li, F., Jin, L., Han, J., Wei, M., and Li, C., 2009, Synthesis and controlled release properties of prednisone intercalated Mg-Al layered double hydroxide composite, *Ind. Eng. Chem. Res.*, 48 (12), 5590–5597.
- [7] Jadam, M.L., Syed Mohamad, S.A., Mohd Zaki, H., Jubri, Z., and Sarijo, S.H., 2021, Antibacterial activity and physicochemical characterization of calcium-aluminium-ciprofloxacin-layered double hydroxide, *J. Drug Delivery Sci. Technol.*, 62, 102314.
- [8] Zhang, Z., Chen, G., and Xu, K., 2013, One-pot green hydrothermal synthesis of stearate-intercalated MgAl layered double hydroxides, *Appl. Clay Sci.*, 72, 206–210.
- [9] Bernardo, M.P., Moreira, F.K.V., and Ribeiro, C., 2017, Synthesis and characterization of eco-friendly Ca-Al-LDH loaded with phosphate for agricultural applications, *Appl. Clay Sci.*, 137, 143–150.
- [10] Rebitski, E.P., Darder, M., and Aranda, P., 2019, Layered double hydroxide/sepiolite hybrid nanoarchitectures for the controlled release of herbicides, *Beilstein J. Nanotechnol.*, 10, 1679–1690.
- [11] Sarijo, S.H., Sheikh Mohd Ghazali, S.A.I., and Hussein, M.Z., 2015, Synthesis of dual herbicides-intercalated hydrotalcite-like nanohybrid compound with simultaneous controlled release property, *J. Porous Mater.*, 22 (2), 473–480.
- [12] Ee, G.C.L., Izzaddin, S.A., Rahmani, M., Sukari, M.A., and Lee, H.L., 2006,  $\gamma$ -Mangostin and rubraxanthone, two potential lead compounds for anti-cancer activity against CEM-SS cell line, *Nat. Prod. Sci.*, 12 (3), 138–143.
- [13] Abdullah, A., Abd Gani, S.S., Mohd Mokhtar, N.F., Taufiq Yap, Y.H., Haiyee, Z., and Mustafa, S., 2018, Supercritical carbon dioxide extraction of red pitaya (*Hylocereus polyrhizus*) seeds: Response surface optimization, fatty acid composition and physicochemical properties, *Malays. Appl. Biol.*, 47 (2), 39–46.
- [14] Mohd Nor, N., Salih, N., and Salimon, J., 2021, Optimization of the ring opening of epoxidized palm oil using D-optimal design, *Asian J. Chem.*, 33 (1), 67–75.
- [15] Sarijo, S.H., Hussein, M.Z., Yahaya, A.H.J., and Zainal, Z., 2010, Effect of incoming and outgoing exchangeable anions on the release kinetics of phenoxyherbicides nanohybrids, *J. Hazard. Mater.*, 182 (1-3), 563–569.
- [16] Abd Ghani, K.D., Nayan, S., Sheikh Mohd Ghazali, S.A.I., Shafie, L.A., and Nayan, S., 2010, Critical internal and external factors that affect firms strategic planning, *Int. Res. J. Finance Econ.*, 51, 50–58.
- [17] Ahmad, R., Hussein, M.Z., Sarijo, S.H., Wan Abdul Kadir, W.R., and Taufiq Yap, Y.H., 2016, Synthesis and characteristics of valeric acid-zinc layered hydroxide intercalation material for insect pheromone controlled release formulation, *J. Mater.*, 2016, 1285721.
- [18] Salleh, N.M., Mohsin, S.M.M., Sarijo, S.H., and Sheikh Mohd Ghazali, S.A.I., 2017, Synthesis and physico-chemical properties of zinc layered hydroxide-4-chloro-2-methylphenoxy acetic acid (ZMCPA) nanocomposite, *IOP Conf. Ser.: Mater. Sci. Eng.*, 204, 012012.
- [19] Hussein, M.Z., Sarijo, S.H., Yahaya, A.H., and Zainal, Z., 2007, Synthesis of 4-chlorophenoxyacetate-zinc-aluminium-layered double hydroxide nanocomposite: Physico-chemical and controlled

- release properties, *J. Nanosci. Nanotechnol.*, 7 (8), 2852–2862.
- [20] Mohd Nor, N., Salih, N., and Salimon, J., 2021, Chemically modified *Jatropha curcas* oil for biolubricant applications, *Hem. Ind.*, 75 (2), 117–128.
- [21] Abdullah, A., Abd Gani, S.S., Taufiq Yap, Y.H., Abdul Haiyee, Z., Zaidan, U.H., Kassim, M.A., and Effendi Halmi, M.I., 2019, Lipase-catalyzed synthesis of red pitaya (*Hylocereus polyrhizus*) seed oil esters for cosmeceutical application: Process optimization using response surface methodology, *RSC Adv.*, 9, 5599–5609.